Antibodies Damage the Resilience of Fimbriae, Causing Them To Be Stiff and Tangled

Bhupender Singh,[a] Narges Mortezaei,[a] Stephen J. Savarino,[b] Bernt Eric Uhlin,[c] Esther Bullitt,[d] Magnus Andersson[a]

Department of Physics, Umeå University, Umeå, Sweden[a]; Enteric Diseases Department, Naval Medical Research Center, Silver Spring, Maryland, USA[b]; Laboratory for Molecular Infection Medicine Sweden (MIMS), Department of Molecular Biology, Umeå University, Umeå, Sweden[c]; Department of Physiology and Biophysics, Boston University School of Medicine, Boston, Massachusetts, USA[d]

ABSTRACT As adhesion fimbriae are a major virulence factor for many pathogenic Gram-negative bacteria, they are also potential targets for antibodies. Fimbriae are commonly required for initiating the colonization that leads to disease, and their success as adhesion organelles lies in their ability to both initiate and sustain bacterial attachment to epithelial cells. The ability of fimbriae to unwind and rewind their helical filaments presumably reduces their detachment from tissue surfaces with the shear forces that accompany significant fluid flow. Therefore, the disruption of functional fimbriae by inhibiting this resilience should have high potential for use as a vaccine to prevent disease. In this study, we show that two characteristic biomechanical features of fimbrial resilience, namely, the extension force and the extension length, are significantly altered by the binding of antibodies to fimbriae. The fimbriae that were studied are normally expressed on enterotoxigenic *Escherichia coli*, which are a major cause of diarrheal disease. This alteration in biomechanical properties was observed with bivalent polyclonal antifimbrial antibodies that recognize major pilin subunits but not with the Fab fragments of these antibodies. Thus, we propose that the mechanism by which bound antibodies disrupt the uncoiling of natural fimbria under force is by clamping together layers of the helical filament, thereby increasing their stiffness and reducing their resilience during fluid flow. In addition, we propose that antibodies tangle fimbriae via bivalent binding, i.e., by binding to two individual fimbriae and linking them together. Use of antibodies to disrupt physical properties of fimbriae may be generally applicable to the large number of Gram-negative bacteria that rely on these surface-adhesion molecules as an essential virulence factor.

IMPORTANCE Our study shows that the resiliency of colonization factor antigen I (CFA/I) and coli surface antigen 2 (CS2) fimbriae, which are current targets for vaccine development, can be compromised significantly in the presence of antifimbrial antibodies. It is unclear how the humoral immune system specifically interrupts infection after the attachment of enterotoxigenic *Escherichia coli* (ETEC) to the epithelial surface. Our study indicates that immunoglobulins, in addition to their well-documented role in adaptive immunity, can mechanically damage the resilience of fimbriae of surface-attached ETEC, thereby revealing a new mode of action. Our data suggest a mechanism whereby antibodies coat adherent and free-floating bacteria to impede fimbrial resilience. Further elucidation of this possible mechanism is likely to inform the development and refinement of preventive vaccines against ETEC diarrhea.

KEYWORDS pili, IgG, vaccine, CFA/I, CS2, optical tweezers

Intestinal infections with enterotoxigenic *Escherichia coli* (ETEC) are a major concern for children in resource-limited countries and cause acute diarrhea that can result in death or long-term consequences (1, 2). Travelers are also at risk of ETEC diarrhea (3). Once in the intestine, ETEC adheres to host cells, often facilitated by helical, long, filamentous adhesion fimbriae, and provokes fluid and electrolyte loss through the action of enterotoxins (4). Adherence by means of fimbriae is indeed the critical first step in ETEC pathogenesis. Twenty-five different adherence fimbriae have been identified from clinical isolates of ETEC, including colonization factor antigen I (CFA/I) and coli surface antigen 2 (CS2) (5, 6). For CFA/I and related fimbriae, interaction of a fimbrial tip protein with specific intestinal epithelial receptors initiates bacterial colonization (4). Recent studies suggest that the quaternary structure of a fimbrial shaft plays an additional deterministic role in colonization, inasmuch as the shaft of certain ETEC fimbriae, as well as those of other pathogenic *E. coli*, is adapted to organ-specific biomechanical and structural features. Despite their differences in biogenesis and assembly processes, when analyzed biomechanically, ETEC-expressed fimbriae unwind at a characteristic low-unwinding steady force of <20 pN (7, 8), while fimbriae expressed by extraintestinal pathogenic *E. coli* (ExPEC), such as type 1, P, and S fimbriae, require a steady force of >20 pN to unwind (7, 9–12).

Due to the essential role played by fimbriae in ETEC pathogenesis, they have commonly served as targets for the development of preventive vaccines against ETEC diarrhea (13–15). Recent vaccination strategies involve the use of either multiple colonization factors or a recombinant antigen consisting of multiple fimbrial epitopes (16–18). Use of fimbriae as an immunizing antigen has proven effective in model organisms and in human volunteers challenged with ETEC following passive immunization with an hyperimmune cocktail containing predominantly antifimbrial antibodies (19, 20). While the precise mechanism is unknown, both active and passive immunizations with ETEC fimbrial colonization factors may result in protection by inhibiting bacterial attachment, enhancing bacterial aggregation, and/or opsonization (21–23).

Recent studies have revealed additional potential mechanisms by which antibodies target the bacterial adhesion process. Antiadhesin IgG antibody isotypes mediate neutrophil-dependent clearance of the enteropathogen *Citrobacter rodentium* from rodents (24), and in cases of ETEC and uropathogenic *Escherichia coli* (UPEC), antifimbrial IgGs severely limit the biomechanical resilience of CS20 and P fimbriae, respectively (25, 26). This resilience is important for reducing the force on the adhesin when bacteria are exposed to shearing fluid forces in both intestinal and extraintestinal milieus (27, 28). For example, *E. coli* expressing CFA/I fimbriae with a point mutation in the fimbrial major subunit that disrupts its quaternary helical architecture is unable to aggregate erythrocytes in an *in vitro* model of intestinal adherence (11). However, the extent to which antifimbrial antibodies distort the biomechanical properties of ETEC fimbriae *in vivo* and their consequences on bacterial pathogenesis are not yet known.

RESULTS

Imaging the expression of fimbriae using atomic force microscopy. We used atomic force microscopy (AFM) to monitor the expression, average lengths, and helicity of fimbriae. AFM micrographs in Fig. 1 show uniform distributions of CS2 and CFA/I fimbriae, respectively, attached to *E. coli*. The average lengths (±standard deviations) of CS2 and CFA/I fimbriae were 0.88 ± 0.34 μm (n = 270) and 0.87 ± 0.31 μm (n = 174), respectively. Micrographs show that CS2 and CFA/I fimbriae were primarily in their intact helical form (black arrow in Fig. 1A). Narrow structures representing unwound CS2 fimbriae (yellow arrow in Fig. 1A) were only occasionally observed.

Resilience of CS2 and CFA/I fimbriae. We measured the resilience of CS2 and CFA/I fimbriae under steady-state conditions (0.05 μm/s extension) using the optical tweezers system, as shown in Fig. 2A1 and B1 for individual CS2 and CFA/I fimbriae, respectively. The responses comprised three distinct force regions, which are typical for helical fimbriae, including an increasing force, a constant force, and an increasing force (29). As found from previous studies, the CS2 and CFA/I fimbriae unwound at a constant force
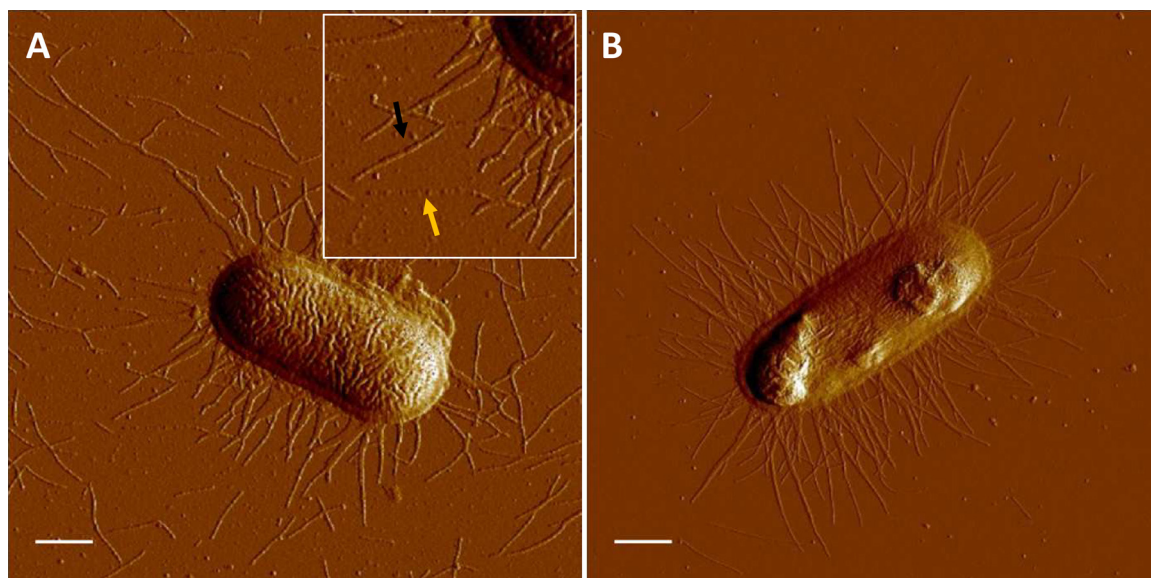
FIG 1 AFM of ETEC cells expressing fimbriae. (A) Micrograph showing a single C91F cell expressing CS2 fimbriae. The black arrow indicates a fimbria in its helical form (wound), whereas the yellow arrow shows an extended (unwound) CS2 fimbria. The inset represents 1.5× magnification of the micrograph in the vicinity of the arrows. (B) Micrograph showing a single BL21-A2/pMAM2 expressing peritrichous CFA/I fimbriae, which were primarily in their helical form (wound). Bars = 0.5 μm.

of 10 pN and 7.5 pN, respectively (8, 12). Occasional multifimbria interactions with the probe bead generated distinct force plateaus, shown as multiples of the force needed to unwind one fimbria (Fig. 2A1 and B1, insets). Fimbriae detached sequentially with extension, and we could always extend the attached fimbriae until only one fimbria
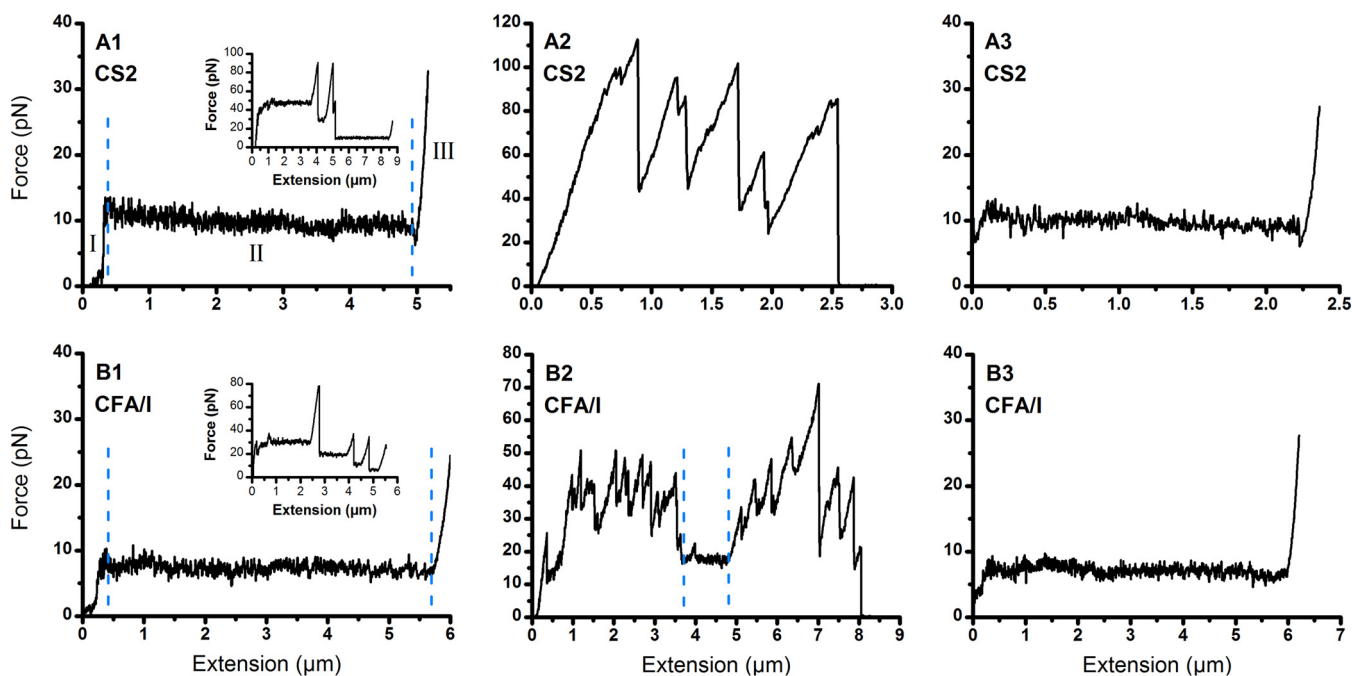
FIG 2 Force spectroscopy on CS2 and CFA/I fimbriae. Force extension responses of CS2 (A1) and CFA/I (B1) fimbriae are shown; insets show the force responses when multiple fimbriae are bound and where distinct force plateaus can be identified. The force responses are divided into three distinct regions: I shows a linear increase of the force, II shows unwinding of the intact quaternary structure of the fimbria, and III shows overstretching of the fimbria after complete unwinding of the quaternary structure. Extension responses of CS2 (A2) and CFA/I (B2) fimbriae in the presence of 2.8 μg/ml purified antifimbrial antibodies are shown. Antibodies significantly altered the force responses of the fimbriae. The small constant plateau between the dashed lines in B2 shows a short unwinding region, which was rarely seen when analyzing all data. Extension responses of CS2 (A3) and CFA/I (B3) fimbriae in the presence of Fab fragments (2.8 μg/ml) are shown. The presence or absence of Fab fragments did not change the force responses (e.g., compare A1 with A3).
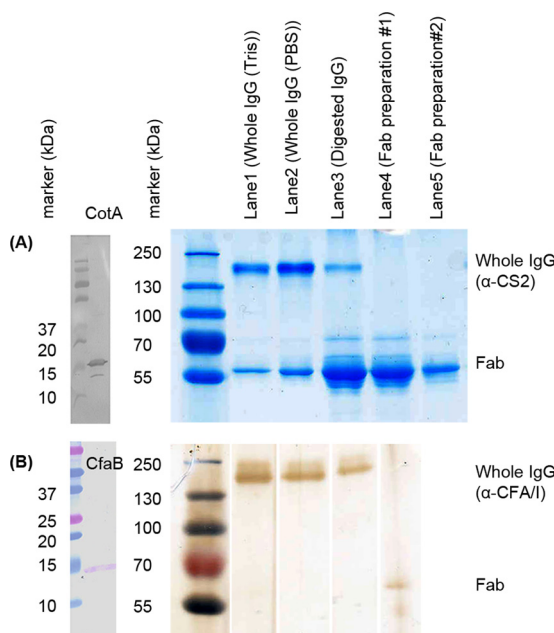
FIG 3 Analysis of antibodies and Fab preparations. (A) Anti-CS2 antibodies and Fab fragments are shown. (left) Western blot of purified CS2 fimbriae using anti-CS2 antisera (R1590) indicating a specific band for the major structural subunit, CotA, at approximately 15 kDa. (right) PageBlue staining after SDS-PAGE of purified anti-CS2 antibodies in Tris buffer (lane 2), purified anti-CS2 antibodies in 1× PBS (lane 3), papain-digested anti-CS2 antisera (lane 4), and purified Fab fractions 1 and 2 in 1× PBS (lanes 5 and 6). Anti-CS2 Fab fraction 2 was used in biomechanical assays. (B) Anti-CFA/I antibodies and Fab fragments are shown. (left) Western blot of purified CFA/I fimbriae using anti-CFA/I antisera (R2175) indicating a specific band for the major structural subunit, CfaB, at approximately 15 kDa. (right) Silver staining after SDS-PAGE of purified anti-CFA/I antibodies in Tris buffer (lane 2), purified anti-CFA/I antibodies in 1× PBS (lane 3), papain-digested anti-CFA/I antisera (lane 4), and purified Fab fraction in 1× PBS (lane 5), which was used in biomechanical assays. Lane 1 shows molecular size markers.

remained attached, which we used to quantify the mechanical properties of a single fimbria.

The characteristic resilience of helical fimbriae, with the capability to unwind to ∼7 times its original length (8, 12) and rewind upon release of tensile force, is shown for CS2 and CFA/I (see Fig. S1 and S2, respectively, in the supplemental material). The unwinding and rewinding curves have a large amount of overlap and indicate that measurements were performed under steady-state conditions and without any external perturbations (8, 12).

Antifimbrial antibodies damage the resilience of CS2 and CFA/I fimbriae. To study the impact of antifimbrial antibodies on the resilience of CS2 and CFA/I fimbriae, we measured spectroscopic force in the presence of purified polyclonal antifimbrial antibodies. Antifimbrial antisera were raised against intact fimbriae with the major structural subunits as the primary antigens. Anti-CS2 and anti-CFA/I antisera were tested by Western blot for their ability to recognize purified CotA and CfaB, the major structural subunits of CS2 and CFA/I fimbriae, respectively (Fig. 3A and B, left). Antibodies purified from the antisera were analyzed by SDS-PAGE, which revealed molecular weights that were consistent with those of IgG class antibodies (Fig. 3A and B, right).

Thereafter, we performed force spectroscopy on CS2 and CFA/I fimbriae in the presence of purified antifimbrial IgG. In preliminary experiments, we found that an IgG concentration of 2.8 μg/ml significantly affected the force extension response (Fig. 2A2), showing only high force peaks and no indication of a region that unwinds under a constant force. It was not possible to rewind the structure at this concentration, as it always detached from the probe bead during extension before a single fimbria could completely extend. This was typical for all experiments performed at 2.8 μg/ml (see Fig.
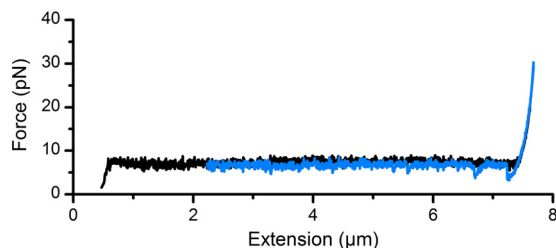
FIG 4 Force-extension responses of CFA/I fimbriae in the presence of antiadhesin antibodies. Black curve represents unwinding and the blue curve represents rewinding of the fimbria.

S3). The IgG concentration was sequentially lowered by 10-fold until a single fimbria extended and a partial rewinding curve was measured. The force-extension data at 0.28 μg/ml is less disrupted than the data at 2.8 μg/ml, but show multiple peaks and that the force never descended to 10 pN, indicating that extension of one single fimbria did not occur (see Fig. S4). Again, it was not possible to rewind the structure since the fimbriae always detached from the bead during the initial extension. Data from experiments at 0.028 μg/ml showed less disruption with only a few minor peaks in the force, and the fimbriae were able to extend to enable identification of a single fimbria. This antibody concentration enabled us to assess a partial rewinding curve (see Fig. S5).

Similar experiments were performed for CFA/I in the presence of 2.8 μg/ml purified polyclonal anti-CFA/I antibodies. Representative force-response profiles are shown in Fig. 2B2 (see also Fig. S6). The data show a high degree of disruption in the force-extension curve. Constant force plateaus were occasionally observed at multiples of the force required to extend a single fimbria. However, it was not possible to unwind a single fimbria nor to measure a rewinding curve. At a 10-fold lower concentration, 0.28 μg/ml, we observed that the force-extension was slightly disrupted and we were able to assess a response from a single fimbria (see Fig. S7).

In addition to alterations in the forces required for unwinding, the extension lengths of fimbriae were also significantly affected in a high concentration of antifimbrial antibodies. This was clearly seen when comparing the representative force-extension curves of CS2 (Fig. 2A1 and A2; also see Fig. S3 and S4). We calculated the average unwinding length, i.e., the length of the force plateau, for all fimbriae in each of the groups. The mean extension lengths of CS2 fimbriae in the absence and presence of antifimbrial antibodies were 5.2 $\pm$ 2.5 μm and 1.5 $\pm$ 0.8 μm ($n = 20$), respectively. These mean values are significantly different (t test, $P = 2.61 \cdot 10^{-7}$).

Intact bivalent antibodies are essential for challenging fimbrial resilience. Next, we determined whether the damage to fimbrial resilience is due to antibodies binding to their specific epitopes or a direct physical intervention. We cleaved the antifimbrial antibodies to monovalent antigen-binding fragments, Fabs. Fabs prepared from anti-CS2 and anti-CFA/I antifimbrial antisera were analyzed by SDS-PAGE (Fig. 3A and B, respectively, right). Force responses of individual CS2 and CFA/I fimbriae in the presence of Fab fragments at 2.8 μg/ml (Fig. 2A3 and B3) show that Fab fragments had an insignificant impact on force-extension curves (cf. Figure 2A2 and B2). That is, the unwinding force did not show a significant change in the presence of Fabs and was very similar to the force response in the absence of antibodies (Fig. 2A1 and B1).

Control measurements using antiadhesin antibodies. To verify that the altered resilience of fimbriae results from the physical interference of antibodies with the fimbrial shaft, we performed force-extension experiments in the presence of a high concentration (85.8 μg/ml) of antibodies raised against the tip adhesin. Using antibodies directed against CfaE, the CFA/I adhesin (Fig. S8 shows Western blot and purified protein analysis), we investigated the biomechanics of the shaft. The force-extension response of CFA/I fimbriae in the presence of antiadhesin antibodies is shown in Fig. 4 and Fig. S9. This antiserum preparation served as a very nice control compared to the antifimbrial antisera, essentially proving that it is the antibodies directed against the major subunit that adversely impact the biomechanical properties of CFA/I.

DISCUSSION

CS2 and CFA/I fimbriae facilitate ETEC colonization in the small intestine. These fimbriae have a helical configuration that can be extended several times their initial length with the application of very low tensile forces, namely, ~10 pN and ~7.5 pN of unwinding force for CS2 and CFA/I fimbriae, respectively, distinguishing them as fimbriae with the lowest required unwinding forces described to date (8, 12). Fimbrial unwinding is proposed to be essential for the initial attachment and sustained adhesion of bacterial cells, since unwinding reduces the load on the adhesin-receptor interaction (27, 28). Therefore, increasing the fimbrial stiffness by inhibiting unwinding might prevent bacteria from initiating and sustaining attachment (25, 26). Since antibodies generated against common ETEC fimbrial colonization factors interact with and significantly reduce the elastic deformation of the fimbriae, those with bound antibodies lose their ability to absorb energy. These findings suggest that antifimbrial antibodies might provide protection against ETEC bacteria by interfering with fimbrial elasticity.

Our data show that resiliency of CS2 and CFA/I fimbriae is significantly diminished by bivalent binding of antifimbrial antibodies, thereby raising the unwinding force severalfold and removing the constant force plateau. To affect fimbrial resilience, antibodies must bind to fimbrial shaft subunits, as our data show that antibodies against the tip adhesins, which do not bind to or compromise the fimbrial shaft, have no impact on fimbrial unwinding. However, it is extremely unlikely that bivalent antibody binding causes elongated fimbriae to become locked in an unwound configuration. While it is sterically possible for an antibody to bind two epitopes on an unwound fimbria, the linker region between the two arms of the antibodies is highly mobile. Similarly, the linker region between the subunits of fimbriae is also mobile. With binding of an antibody to a single epitope, it is extremely unlikely that a second (identical) epitope will be positioned such that the second arm can bind to a nearby subunit. Thus, bivalent binding to unwound fimbriae is not expected to occur, due to both the limited reach of the antibody arms and the combined mobility of the antibody and the fimbria. However, dips in the force were occasionally observed when fimbriae were rewinding. These dips might have been caused by the transient bivalent binding of antibodies to unwound fimbriae.

The importance of bivalent binding was also demonstrated by the lack of impact that Fab fragments had on fimbrial biomechanics (Fig. 2A3 and B3). Thus, we conclude that both bivalent and shaft-specific antibodies are required to cross-link and lock together layers in the shaft, and that these antibodies thereby reduce fimbrial resilience.

We propose that the high extension forces measured in the presence of antifimbrial antibodies resulted from both intrafimbrial cross-linking, i.e., the binding of two subunits on the same fimbria, and to some extent, interfimbrial cross-linking, i.e., the binding of two fimbriae. We speculate that interfimbrial cross-linking might also change the resilience of fimbriae, since this situation is similar to that when connecting two parallel springs with a stiff linker. If one spring is extended with an external force, it will abruptly increase the spring constant when the linker (in this case an antibody) connecting the two springs is fully stretched. This would lead to a transient increase in the force, significantly reducing the lifetime of the receptor-ligand bond and most likely lead to bond breakage (30).

Secretory IgA and, to a much lower extent, IgM provide the first line of immune defense in the intestine and luminal surfaces (31, 32). With this in mind, we conceptually modeled a plausible situation at the brush border of the small intestine in the absence and presence of antibodies, as described in Fig. 5A. ETEC bacteria are attached to microvilli with adhesion fimbriae and exposed to peristaltic movements and fluid flow from the lumen (33, 34). The movement of the microvilli will in turn apply stress to fimbriae and the receptor-ligand bond. However, the fimbrial resilience will modulate and effectively dampen transients in the force prolonging the lifetime of the
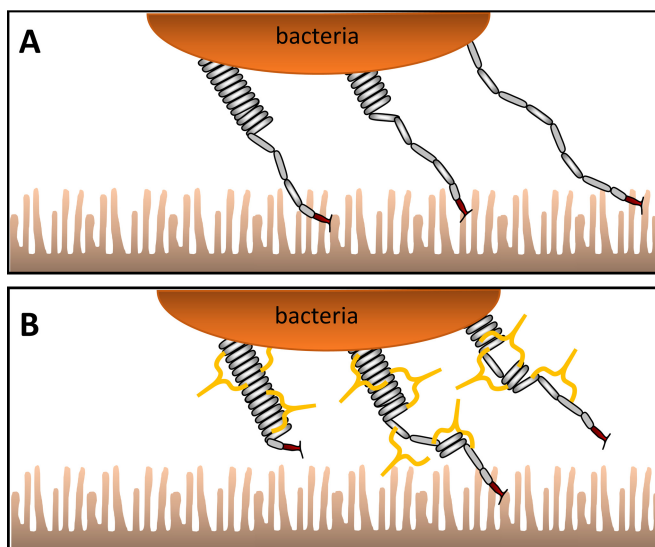
FIG 5 Conceptual model of fimbriated bacteria in the intestine. (A) Fimbriae in the absence of antibodies bind to microvilli and unwind when exposed to forces of the intestinal fluid flow. (B) Fimbriae decorated with antibodies cannot freely unwind and rewind, thereby limiting sustained binding to microvilli.

receptor-ligand bond (30). In contrast, in the presence of antibodies (Fig. 5B), primarily secretory IgA, there are two possibilities. Either the antibodies attach to fimbriae and increase fimbrial stiffness or the presence of antibodies results in fimbrial tangles. In either scenario, the function of these antibody-decorated fimbriae is now impeded by the transient forces from the lumen, which can break the receptor-ligand bond and flush the bacterium from the intestine. Once a bacterium is detached from the surface, antibodies attached to the fimbriae will limit the ability to reattach, resulting in reduced bacterial retention in the intestine.

As common bacterial surface antigens with essential roles in initiating and sustaining intestinal attachment, fimbrial colonization factors of ETEC have been included as primary components of several ETEC vaccines in clinical evaluations (17, 19, 20). Recent work has suggested that the CfaE minor tip-localized adhesin of CFA/I serves as a protective vaccine against ETEC disease in a neonatal mouse model on the basis of an antibody response that inhibits adhesin-receptor binding (35). The combination of the biomechanistic framework presented here and prior evidence showing that the protection from antibodies against purified CFA/I fimbriae (20) is predominantly due to a response against the major stalk-forming subunit leads to a new hypothesis: the optimal subunit for an ETEC vaccine will elicit robust responses to both the CfaE adhesin and the CfaB stalk-forming subunits. A previously described CfaE-CfaB fusion protein (11) represents such an antigen that could be used to test this hypothesis.

Our current study shows that the resiliency of CFA/I and CS2 fimbriae, which are current targets for vaccine development and require extremely low unwinding forces, can be compromised significantly in the presence of antifimbrial antibodies. It is unclear how the humoral immune system specifically interrupts infection after the attachment of ETEC to the epithelial surface. Our study indicates that immunoglobulins, in addition to their well-documented role in adaptive immunity, can mechanically damage the resilience of fimbriae of surface-attached ETEC, thereby revealing a new mode of action. Our data suggest a mechanism whereby antifimbrial antibodies coat adherent and free-floating bacteria in such a manner as to mechanically impede fimbrial resilience. Further elucidation of this possible mechanism is likely to inform the development and refinement of preventive vaccines and therapeutics against ETEC diarrhea.

MATERIALS AND METHODS

Bacterial strains. *E. coli* strain BL21-A2/pMAM2 expressing CFA/I fimbriae were grown to an optical density at 600 nm (OD_{600}) of 0.5 and CFA/I expression was induced for 6 h with arabinose (36). *E. coli*

strain C91F expressing CS2 fimbriae (37) was grown overnight on colonization factor antigen (CFA) agar plates at 37°C and passaged for another overnight growth. Fimbrial expression was visualized by atomic force microscopy (AFM).

Raising of antisera against CFA/I and CS2 fimbriae. CFA/I and CS2 fimbriae from strains WS1933D and C91F, respectively, were purified by heat extraction and then precipitated with ammonium sulfate (38). Antifimbrial antisera (Envigo) were raised by Harlan Laboratories, Inc. Anti-CS2 (R1590) and anti-CFA/I (R2175) polyclonal antisera predominantly recognized the major subunits CotA and CfaB of CS2 and CFA/I, respectively, as shown by Western blot analysis against purified CS2 and CFA/I fimbriae isolated from C91F and BL21-A2/pMAM2 strains using a 15% polyacrylamide gel (for SDS-PAGE) and immunoblotting with anti-CS2 (1:10^6 dilution) and anti-CFA/I (1:10^7 dilution) antisera.

CfaB and the adhesin CfaE of the CFA/I operon in strain WS1933D share 100% identity with those in the CFA/I operon in strain E7473/0, which was cloned into pMAM2 and used in these studies.

Antibody purification and Fab fragment preparation. Polyclonal IgG antibodies were purified using the Amicon Pro affinity concentration kit-protein A (Amicon) according to the manufacturer's instructions. To obtain Fab fragments, antibodies were cleaved using the Pierce Fab preparation kit (44985; Pierce) (25). Purified antibodies and Fab fragments were analyzed by electrophoresis under nonreducing and nonboiled conditions using 12% SDS-PAGE. Gels containing anti-CS2 antibodies and Fab fragments were stained with PageBlue (24620; Thermo Fisher Scientific). Due to low protein concentrations, gels containing anti-CFA/I antibodies and Fab fragments were silver stained using the ProteoSilver Plus silver stain kit (PROTSIL1-1KT; Sigma Life Science). The gel was first fixed with a solution containing 50% methanol and 10% acetic acid for 20 min, and then washed first with 30% ethanol and then with water. The gel was stained with silver stain and developed using solutions provided in the kit. Protein concentrations were determined using a NanoDrop spectrophotometer at a wavelength of 280 nm with an extinction coefficient of 14.0 for IgGs and Fab fragments.

Atomic force microscopy. For AFM, 10 μl of bacterial cell suspension in Milli-Q water was placed onto a cleaved ruby red mica sheet (Goodfellow Cambridge, Ltd.), incubated for 5 min at room temperature, and then placed into a desiccator for ~2 h. Micrographs were recorded in ScanAsyst mode using a Nanoscope V Multimode8 AFM setup (Bruker software) with a Bruker ScanAsyst-air probe oscillated at a resonant frequency of 50 to 90 kHz (39). The lengths of fimbriae were assessed using ImageJ software as previously described (12).

Optical tweezers instrumentation. Force spectroscopy was performed using an optical tweezers (OT) setup as previously described (40, 41). Briefly, probe beads and bacterial cells were trapped with an Nd:YVO$_4$ (1,064 nm) laser in continuous-wave mode. The trapped bead position was probed with a HeNe laser (632.8 nm) using a position-sensitive detector. A single bacterium or a probe bead (2.5 μm in diameter) was trapped and positioned with nanometer precision via a computer-controlled piezo stage. Setup optimization was as described in reference 42, and data were analyzed using the Allan variance method (43).

Sample preparation and force spectroscopy measurements. An in-house flow chamber system provided defined conditions for force spectroscopy measurements as previously described (25). A bacterial cell suspension in phosphate-buffered saline (PBS; pH 7.4) was diluted to a concentration expected to have at most one bacterium per field-of-view during experiments. Bacterial cells (4 μl) and surfactant-free 2.5-μm white amidine polystyrene beads (3-2600; Invitrogen) with and without antibodies or Fab fragments were injected into the flow chamber and sealed with a coverslip.

A trapped bacterium was mounted on the side of a poly L-lysine-coated 9.5 μm bead and a 2.5-μm bead was trapped. The trap stiffness was calibrated using the power spectrum method (44). The trapped bead was brought into proximity of the mounted bacterium and attached nonspecifically via a fimbria. The piezo stage was moved using a home-designed LabView program to unwind and rewind the fimbria under steady-state conditions (software available upon request).

A detailed description of the optical tweezers experiments is given in the supplemental materials.

SUPPLEMENTAL MATERIAL

ACKNOWLEDGMENTS

REFERENCES

1. Kotloff KL, Nataro JP, Blackwelder WC, Nasrin D, Farag TH, Panchalingam S, Wu Y, Sow SO, Sur D, Breiman RF, Faruque AS, Zaidi AK, Saha D, Alonso PL, Tamboura B, Sanogo D, Onwuchekwa U, Manna B, Ramamurthy T, Kanungo S, Ochieng JB, Omore R, Oundo JO, Hossain A, Das SK, Ahmed S, Qureshi S, Quadri F, Adegbola RA, Antonio M, Hossain MJ, Akinsola A, Mandomando I, Nhampossa T, Acácio S, Biswas K, O'Reilly CE, Mintz ED, Berkeley LY, Muhsen K, Sommerfelt H, Robins-Browne RM, Levine MM. 2013. Burden and aetiology of diarrhoeal disease in infants and young children in developing countries (the Global Enteric Multicenter Study, GEMS): a prospective, case-control study. Lancet 382:209–222. https://doi.org/10.1016/S0140-6736(13)60844-2.

2. Lanata CF, Fischer-Walker CL, Olascoaga AC, Torres CX, Aryee MJ, Black RE, Child Health Epidemiology Reference Group of the World Health Organization and UNICEF. 2013. Global causes of diarrheal disease mortality in children <5 years of age: a systematic review. PLoS One 8:e72788. https://doi.org/10.1371/journal.pone.0072788.

3. Lozano R, Naghavi M, Foreman K, Lim S, Shibuya K, Aboyans V, Abraham J, Adair T, Aggarwal R, Ahn SY, Alvarado M, Anderson HR, Anderson LM, Andrews KG, Atkinson C, Baddour LM, Barker-Collo S, Bartels DH, Bell ML, Benjamin EJ, Bennett D, Bhalla K, Bikbov B, Bin Abdulhak A, Birbeck G, Blyth F, Bolliger I, Boufous S, Bucello C, Burch M, Burney P, Carapetis J, Chen H, Chou D, Chugh SS, Coffeng LE, Colan SD, Colquhoun S, Colson KE, Condon J, Connor MD, Cooper LT, Corriere M, Cortinovis M, de Vaccaro KC, Couser W, Cowie BC, Criqui MH, Cross M, Dabhadkar KC, et al. 2012. Global and regional mortality from 235 causes of death for 20 age groups in 1990 and 2010: a systematic analysis for the Global Burden of Disease study 2010. Lancet 380:2095–2128. https://doi.org/10.1016/S0140-6736(12)61728-0.

4. Fleckenstein JM, Hardwidge PR, Munson GP, Rasko DA, Sommerfelt H, Steinsland H. 2010. Molecular mechanisms of enterotoxigenic Escherichia coli infection. Microbes Infect 12:89–98. https://doi.org/10.1016/j.micinf.2009.10.002.

5. Anantha RP, McVeigh AL, Lee LH, Agnew MK, Cassels FJ, Scott DA, Whittam TS, Savarino SJ. 2004. Evolutionary and functional relationships of colonization factor antigen I and other class 5 adhesive fimbriae of enterotoxigenic Escherichia coli. Infect Immun 72:7190. https://doi.org/10.1128/IAI.72.12.7190-7201.2004.

6. Nada RA, Shaheen HI, Khalil SB, Mansour A, El-Sayed N, Touni I, Weiner M, Armstrong AW, Klena JD. 2011. Discovery and phylogenetic analysis of novel members of class b enterotoxigenic Escherichia coli adhesive fimbriae. J Clin Microbiol 49:1403–1410. https://doi.org/10.1128/JCM.02006-10.

7. Mortezaei N, Epler CR, Shao PP, Shirdel M, Singh B, McVeigh A, Uhlin BE, Savarino SJ, Andersson M, Bullitt E. 2015. Structure and function of enterotoxigenic Escherichia coli fimbriae from differing assembly pathways. Mol Microbiol 95:116–126. https://doi.org/10.1111/mmi.12847.

8. Andersson M, Björnham O, Svantesson M, Badahdah A, Uhlin BE, Bullitt E. 2012. A structural basis for sustained bacterial adhesion: biomechanical properties of CFA/I pili. J Mol Biol 415:918–928. https://doi.org/10.1016/j.jmb.2011.12.006.

9. Andersson M, Fällman E, Uhlin BE, Axner O. 2006. A sticky chain model of the elongation and unfolding of Escherichia coli P pili under stress. Biophys J 90:1521–1534. https://doi.org/10.1529/biophysj.105.074674.

10. Andersson M, Uhlin BE, Fällman E. 2007. The biomechanical properties of E. coli pili for urinary tract attachment reflect the host environment. Biophys J 93:3008–3014. https://doi.org/10.1529/biophysj.107.110643.

11. Li Y-F, Poole S, Nishio K, Jang K, Rasulova F, McVeigh A, Savarino SJ, Xia D, Bullitt E. 2009. Structure of CFA/I fimbriae from enterotoxigenic Escherichia coli. Proc Natl Acad Sci U S A 106:10793–10798. https://doi.org/10.1073/pnas.0812843106.

12. Mortezaei N, Singh B, Zakrisson J, Bullitt E, Andersson M. 2015. Biomechanical and structural features of CS2 fimbriae of enterotoxigenic Escherichia coli. Biophys J 109:49–56. https://doi.org/10.1016/j.bpj.2015.05.022.

13. Bourgeois AL, Wierzba TF, Walker RI. 2016. Status of vaccine research and development for enterotoxigenic Escherichia coli. Vaccine 34:2880–2886. https://doi.org/10.1016/j.vaccine.2016.02.076.

14. Lundgren A, Bourgeois L, Carlin N, Clements J, Gustafsson B, Hartford M, Holmgren J, Petzold M, Walker R, Svennerholm AM. 2014. Safety and immunogenicity of an improved oral inactivated multivalent enterotoxigenic Escherichia coli (ETEC) vaccine administered alone and together

with dmLT adjuvant in a double-blind, randomized, placebo-controlled phase I study. Vaccine 32:7077–7084. https://doi.org/10.1016/j.vaccine.2014.10.069.

15. Darsley MJ, Chakraborty S, DeNearing B, Sack DA, Feller A, Buchwaldt C, Bourgeois AL, Walker R, Harro CD. 2012. The oral, live attenuated enterotoxigenic Escherichia coli vaccine ACE527 reduces the incidence and severity of diarrhea in a human challenge model of diarrheal disease. Clin Vaccine Immunol 19:1921–1931. https://doi.org/10.1128/CVI.00364-12.

16. Tobias J, Svennerholm AM, Holmgren J, Lebens M. 2010. Construction and expression of immunogenic hybrid enterotoxigenic Escherichia coli CFA/I and CS2 colonization fimbriae for use in vaccines. Appl Microbiol Biotechnol 87:1355–1365. https://doi.org/10.1007/s00253-010-2577-4.

17. Holmgren J, Bourgeois L, Carlin N, Clements J, Gustafsson B, Lundgren A, Nygren E, Tobias J, Walker R, Svennerholm AM. 2013. Development and preclinical evaluation of safety and immunogenicity of an oral ETEC vaccine containing inactivated E. coli bacteria overexpressing colonization factors CFA/I, CS3, CS5 and CS6 combined with a hybrid LT/CT B subunit antigen, administered alone and together with dmLT adjuvant. Vaccine 31:2457–2464. https://doi.org/10.1016/j.vaccine.2013.03.027.

18. Ruan X, Sack DA, Zhang W. 2015. Genetic fusions of a CFA/I/II/IV MEFA (multiepitope fusion antigen) and a toxoid fusion of heat-stable toxin (STa) and heat-labile toxin (LT) of enterotoxigenic Escherichia coli (ETEC) retain broad anti-CFA and antitoxin antigenicity. PLoS One 10:e0121623. https://doi.org/10.1371/journal.pone.0121623.

19. Svennerholm AM, Wenneras C, Holmgren J, McConnell MM, Rowe B. 1990. Roles of different coli surface antigens of colonization factor antigen II in colonization by and protective immunogenicity of enterotoxigenic Escherichia coli in rabbits. Infect Immun 58:341–346.

20. Freedman DJ, Tacket CO, Delehanty A, Maneval DR, Nataro J, Crabb JH. 1998. Milk immunoglobulin with specific activity against purified colonization factor antigens can protect against oral challenge with enterotoxigenic Escherichia coli. J Infect Dis 177:662–667. https://doi.org/10.1086/514227.

21. Neutra MR, Kozlowski PA. 2006. Mucosal vaccines: the promise and the challenge. Nat Rev Immunol 6:148–158. https://doi.org/10.1038/nri1777.

22. Holmgren J, Svennerholm AM. 2012. Vaccines against mucosal infections. Curr Opin Immunol 24:343–353. https://doi.org/10.1016/j.coi.2012.03.014.

23. Qadri F, Ahmed F, Ahmed T, Svennerholm AM. 2006. Homologous and cross-reactive immune responses to enterotoxigenic Escherichia coli colonization factors in Bangladeshi children. Infect Immun 74:4512–4518. https://doi.org/10.1128/IAI.00474-06.

24. Kamada N, Sakamoto K, Seo S-U, Zeng MY, Kim Y-G, Cascalho M, Vallance BA, Puente JL, Núñez G. 2015. Humoral immunity in the gut selectively targets phenotypically virulent attaching-and-effacing bacteria for intraluminal elimination. Cell Host Microbe 13:617–627. https://doi.org/10.1016/j.chom.2015.04.001.

25. Mortezaei N, Singh B, Bullitt E, Uhlin BE, Andersson M. 2013. P-fimbriae in the presence of anti-PapA antibodies: new insight of antibodies action against pathogens. Sci Rep 3:3393. https://doi.org/10.1038/srep03393.

26. Singh B, Mortezaei N, Uhlin BE, Savarino SJ, Bullitt E, Andersson M. 2015. Antibody-mediated disruption of the mechanics of CS20 fimbriae of enterotoxigenic Escherichia coli. Sci Rep 5:13678. https://doi.org/10.1038/srep13678.

27. Miller E, Garcia T, Hultgren SJ, Oberhauser AF. 2006. The mechanical properties of E. coli type 1 pili measured by atomic force microscopy techniques. Biophys J 91:3848–3856. https://doi.org/10.1529/biophysj.106.088989.

28. Zakrisson J, Wiklund K, Axner O, Andersson M. 2012. Helix-like biopolymers can act as dampers of force for bacteria in flows. Eur Biophys J 41:551–560. https://doi.org/10.1007/s00249-012-0814-8.

29. Axner O, Björnham O, Castelain M, Koutris E, Schedin S, Fällman E, Andersson M. 2010. Unraveling the secrets of bacterial adhesion organelles using single molecule force spectroscopy, p 337–362. In Gräslund A, Rigler R, Widengren J (ed), Springer series in chemical physics: single molecule spectroscopy in chemistry, physics and biology. Springer, Berlin, Heidelberg, Germany.

30. Zakrisson J, Wiklund K, Axner O, Andersson M. 2013. The shaft of the type 1 fimbriae regulates an external force to match the FimH catch bond. Biophys J 104:2137–2148. https://doi.org/10.1016/j.bpj.2013.03.059.

31. Brandtzaeg P, Johansen FE. 2005. Mucosal B cells: phenotypic characteristics, transcriptional regulation, and homing properties. Immunol Rev 206:32–63. https://doi.org/10.1111/j.0105-2896.2005.00283.x.

32. Hansen GH, Niels-Christiansen LL, Immerdal L, Danielsen EM. 2006. Antibodies in the small intestine: mucosal synthesis and deposition of anti-glycosyl IgA, IgM, and IgG in the enterocyte brush border. Am J Physiol Gastrointest Liver Physiol 291:G82–G90. https://doi.org/10.1152/ajpgi.00021.2006.

33. Jeffrey B, Udaykumar HS, Schulze KS. 2003. Flow fields generated by peristaltic reflex in isolated guinea pig ileum: impact of contraction depth and shoulders. Am J Physiol Gastrointest Liver Physiol 285:G907–G918. https://doi.org/10.1152/ajpgi.00062.2003.

34. Otto M. 2014. Physical stress and bacterial colonization. FEMS Microbiol Rev 38:1250–1270. https://doi.org/10.1111/1574-6976.12088.

35. Luiz WB, Rodrigues JF, Crabb JH, Savarino SJ, Ferreira LC. 2015. Maternal vaccination with a fimbrial tip adhesin and passive protection of neonatal mice against lethal human enterotoxigenic Escherichia coli challenge. Infect Immun 83:4555–4564. https://doi.org/10.1128/IAI.00858-15.

36. Li Y-F, Poole S, Rasulova F, McVeigh AL, Savarino SJ, Xia D. 2007. A receptor-binding site as revealed by the crystal structure of CfaE, the colonization factor antigen I fimbrial adhesin of enterotoxigenic Escherichia coli. J Biol Chem 282:23970–23980. https://doi.org/10.1074/jbc.M700921200.

37. Smyth CJ. 1982. Two mannose-resistant haemagglutinins on enterotoxigenic Escherichia coli of serotype O6:K15:H16 or H-isolated from travellers' and infantile diarrhoea. J Gen Microbiol 128:2081–2096. https://doi.org/10.1099/00221287-128-9-2081.

38. Chattopadhyay S, Tchesnokova V, McVeigh A, Kisiela DI, Dori K, Navarro A, Sokurenko EV, Savarino SJ. 2012. Adaptive evolution of class 5 fimbrial genes in enterotoxigenic Escherichia coli and its functional consequences. J Biol Chem 287:6150–6158. https://doi.org/10.1074/jbc.M111.303735.

39. Balsalobre C, Morschhäuser J, Jass J, Hacker J, Uhlin BE. 2003. Transcriptional analysis of the sfa determinant revealing multiple mRNA processing events in the biogenesis of S fimbriae in pathogenic Escherichia coli. J Bacteriol 185:620–629. https://doi.org/10.1128/JB.185.2.620-629.2003.

40. Axner O, Andersson M, Björnham O, Castelain M, Klinth JE, Koutris E, Schedin S. 2011. Assessing bacterial adhesion on an individual adhesin and single pili level using optical tweezers, p 301–313. In Linke D, Goldman A (ed), Bacterial adhesion, 1st ed. Springer Verlag, Berlin, Germany.

41. Fällman E, Schedin S, Jass J, Andersson M, Uhlin BE, Axner O. 2004. Optical tweezers based force measurement system for quantitating binding interactions: system design and application for the study of bacterial adhesion. Biosens Bioelectron 19:1429–1437. https://doi.org/10.1016/j.bios.2003.12.029.

42. Andersson M, Fällman E, Uhlin BE, Axner O. 2006. Force measuring optical tweezers system for long time measurements of P pili stability, p 286–295. In Imaging, manipulation, and analysis of biomolecules, cells, and tissues IV, 6088. Proceedings of SPIE–the International Society for Optical Engineering, San Jose, CA. https://doi.org/10.1117/12.642266.

43. Andersson M, Czerwinski F, Oddershede LB. 2011. Optimizing active and passive calibration of optical tweezers. J Opt 13:044020. https://doi.org/10.1088/2040-8978/13/4/044020.

44. Tolić-Nørrelykke SF, Schäffer E, Howard J, Pavone FS, Jülicher F, Flyvbjerg H. 2006. Calibration of optical tweezers with positional detection in the back focal plane. Rev Sci Instrum 77:103101. https://doi.org/10.1063/1.2356852.